CHARACTERIZATION AND H$_2$-STORAGE CAPACITY OF SURFACE-MODIFIED MULTI-WALL CARBON NANOTUBES

Kuen-Song Lin*, Ze-Ping Wang, and Su-Wei Chi
Department of Chemical Engineering and Materials Science/Fuel Cell Center, Yuan Ze University, Chungli City, Taoyuan County, Taiwan 320, R.O.C.

Abstract

The synthesis and identification of multi-wall carbon nanotubes (MWCNTs) and H$_2$ storage capacity of MWCNTs were investigated in the present study. Experimentally, the MWCNTs were produced from the catalytic-assembly benzene-thermal routes by reduction of C$_6$Cl$_6$ with metallic K or Na in the presence of Co/Ni catalyst precursors at 503-623 K for 12 h. The average diameters of K- and Na-MWCNTs were 50 and 60 nm, respectively. The XRD patterns indicated that the abstraction of Cl from C$_6$Cl$_6$ and formation of the KCl or NaCl were involved in the early stage for the synthesis process of MWCNTs. These results may offer a further explanation of how the yield and structure of MWCNTs formed by solvothermal route depend on the Co/Ni catalysts. However, this result indicated that the MWCNTs having Co/Ni particles exist clearly, which may suggest that the Co/Ni particles are also responsible for the nucleation of the MWCNTs. The H$_2$ storage capacity of MWCNTs improved by Pd or NaAlH$_4$ ranged from 2.5-3.5 wt%. From XANES spectra, the Co/Ni catalyst precursors were all metallic Co or Ni nanoparticles. The EXAFS spectra also showed that the Pd or PdCl$_2$ possess a Pd-Pd or Pd-Cl bond distance of 2.76 or 2.25 Å with a coordination number of 6 or 2, respectively. Therefore, Pd nanoparticles are well dispersed on MWCNTs, which may improve the H$_2$ storage capacity significantly.

Introduction

Carbon nanotubes (CNTs) synthesized in the arc-discharge apparatus were first discovered by Iijima in 1991 as nested structures of concentric shells (Iijima, 1991). This stimulated a worldwide research effort to improve their synthesis, structure determination, and physical property calculations and identification (Iijima, 1991). The unique carbon nanotubes are predicted to possess novel mechanical and electrical properties due to their regular, periodic structure and quantum size (Dresselhaus et al., 1995; Dillon et al., 1997; Hone et al., 1999). These properties suggest enormous potential applications for CNTs such as novel nanoscale electronic devices, tips for scanning probe microscopy, hydrogen storage media, reinforcing materials for carbon matrix composites, and catalyst supports (Dillon et al., 1997; Hone et al., 1999; Tong et al., 2002). Realization of these commercial scale uses will require scaleable, economical synthesis methods.

In the recent years, synthesizing of metal-catalyzed CNTs has been pursued by verity of methods, including laser or arc evaporation of a metal graphite composite target, hydrocarbon pyrolysis or CO disproportionation on a metal catalyst in high temperatures (Guo et al., 1995; Jiang et al., 2000; Wang et al., 2002, Sun et al. 2002; Liu et al., 2003). The laser or arc evaporation provides a modest control over process conditions, thus producing many undesired by-products, low yields, and acquire physical separation challenges (Chen et al., 1998; Wong et al., 1998; Hamon et al., 2001; Zhang et al., 2003; Branca et al., 2004). In contrast, high temperature furnaces offer a high degree of control over the hydrocarbon identity, temperature, and reaction time, all of which can be optimized for product purity (Mickelson et al., 1998; Bahr et al., 2001; Xing et al., 2005). However, these methods are energy intensive and produce relatively low quantities of CNTs. In addition, neither method is readily scaleable for bulk commercial production. Conversely, a novel catalytic-assembly benzene-solvothermal route to MWCNTs, by a reduction of hexachlorobenzene on metallic K in the presence of Co/Ni catalyst in an autoclave, has been used (Jiang et al., 2000; Wang et al., 2002). The reaction temperature of this CNTs synthesis system is much lower than that of others. The valency and fine structure of Co and Ni atom used as the catalyst precursor of CNTs formation have also not been well studied. The concurrence of Co/Ni metal nanoparticles nucleation and CNTs growth within a reactive hydrocarbon atmosphere creates a complex transient chemical environment, making it difficult to study the inception and growth processes in CNTs synthesis (Jiang et al., 2000; Wang et al., 2002).

Complex metal hydrides, with the form ABH$_4$, where A is one of the alkali metals, and B is a group III atom, have been widely studied in solution as proton acceptors for enhancement of H$_2$ adsorption abilities (Moc et al., 2003; Ross et al., 2004; Wang and Jensen, 2004; Chaudhuri and Muckerman, 2005; Majzoub et al., 2005; Pukazhselvan et al., 2005; Wang et al., 2005a; 2005b). In view of the increasing interest in NaAlH$_4$ as a viable hydrogen storage material, this alternative material is particularly admixed with non-metallic, lightweight, and high-surface-area CNTs. The CNTs are known to possess significant catalytic activity via the π and σ bonds (Iijima 1991; Dresselhaus et al., 1995; Dillon et al., 1997; Hone et al., 1999). XANES/EXAFS spectroscopy was used to investigate the valency and fine structure of these complex metals in the synthesis of CNTs. The XANES/EXAFS spectra offer a basic understanding of the oxidation states and fine structures of Pd, Co and Ni atoms in the complex catalytic precursor. Therefore the further study of the dispersion and interaction mechanism

of these metals on CNTs may be investigated. XANES/EXAFS spectroscopy is also an excellent technique for characterizing the valency and local structure of Pd/Co/Ni metals in the catalyst precursor with short-range order (Conradson, 1998; Vlaic et al., 1998; Koningsberger et al., 1999; Lytle, 1999). Thus, the main objectives of the present study were to investigate the fine structures, oxidation states or surface chemical modification of MWCNTs and Pd/Co/Ni atoms dispersed in the catalyst precursor by TEM, XRPD, EDS or XANES/EXAFS spectroscopy. The adsorptive H_2 storage capacity of MWCNTs, improved by dopping Pd or $NaAlH_4$, was also studied.

Experimental

The MWCNTs synthesis was conducted in a batch system. Benzene (100 mL) was placed into a 250 ml PTFE-lined stainless steel 316 autoclave. Then 15 g hexachlorobenzene and 20 g metallic potassium were added. Subsequently 70-80% of the autoclave's capacity was filled with 15 mL of benzene and 700 mg of catalyst precursors. The catalyst precursor was prepared by dissolving 1 g of $CoCl_2 \cdot 6H_2O$ and $NiCl_2 \cdot 6H_2O$ mixture (mole ratio Co/Ni = 1) in 100 mL of absolute ethanol, followed by drying at 353 K and calcining at 423 K in a flowing air. All the chemicals used are high-purity (ACS grade). The sealed autoclave was heated in the furnace at 503-623 K for 8-12 h, and then cooled to room temperature. The samples obtained were repeatedly and sequentially washed with absolute ethanol, dilute acid, and de-ionized double distilled water to remove the residual impurities, such as chlorides and remaining catalyst. Finally, the samples were vacuum-dried at 343-353 K for 6-10 h. The well-dispersed Pd/MWCNTs were prepared by adding MWCNTs into $PdCl_{2(aq)}$ for dispersion or impregnation and dried in alcohol solution at 323 K. Finally, the PdO/MWCNTs were reduced to form the active Pd/MWCNTs with flowing hydrogen gases at 393-413 K. In addition, adsorptive hydrogen storage efficiency of MWCNTs was measured by a gravimetric analyzer at 298 K and 1-5 atm.

In order to more thoroughly examine the H_2 adsorption efficiencies on K-MWCNTs, batch adsorption experiments were conducted at 298 K. The average Co/Ni metal contents in the catalyst precursor were evaluated by atomic absorption spectroscopy (AAS, GBC model 908) and induced couple plasma/mass spectroscopy (ICP/MS, ELAN model 5000). Each calibration curve was generated with its corresponding standard metal solution at ten different concentrations and that generated the expected Co/Ni metal concentrations in the catalysts. Concentrations of Co/Ni in the catalyst precursors were then calculated. The morphologies of the samples were observed with a Model Zeiss 10C transmission electron microscope (TEM) at 200 kV, and the microstructures of MWCNTs were measured with a JEOL 2010 high-resolution transmission electron microscope (HRTEM) also at 200 kV. Samples for the electron microscope were prepared by 1 h ultrasonic dispersion of 0.2 g of product with 50 mL of absolute ethanol in a 100 mL conical flask. Then a drop of the solution was placed on a copper microgrid or carbon film and dried in air before observation. Structures of the MWCNTs or Co/Ni precursors samples were measured by X-ray powder diffraction (XRD) scanned from 10 to 90°(2θ) with a scan rate of 4°(2θ)/min with monochromatic CuK_α radiation (MAC Science, MXP18).

The XANES/EXAFS spectra were collected at 01C1 or the Wiggler 17C1 beamline at the National Synchrotron Radiation Research Center (NSRRC) of Taiwan. The electron storage ring was operated with an energy of 1.5 GeV and a current of 100-200 mA. A Si(111) DCM was used for providing highly monochromatized photon beams with energies of 1 to 15 keV and resolving power (E/ΔE) of up to 7000. Data were collected in fluorescence or transmission mode with a Lytle ionization detector (Lytle, 1999) for Pd (26711 eV), Co (7709 eV) and Ni (8333 eV) K edge experiments at room temperature. The photon energy was calibrated by characteristic preedge peaks in the absorption spectra of Pd, Co and Ni standards. The raw absorption data in the region of 50 to 200 eV below the edge position were fit to a straight line using the least-square algorithms. The XANES extend to an energy of the order of 50 eV above the edge. The k^2-weighted and EXAFS spectra were Fourier transformed to R space over the range between 2.5 and 12.5 $Å^{-1}$. The EXAFS data were analyzed by using the UWXAFS 3.0 program and FEFF 8.0 codes (Conradson et al., 1998; Vlaic et al., 1998; Koningsberger et al., 1999).

Results and discussion

The TEM microphotographs were used to investigate the morphologies, crystallinity, and microstructures of MWCNTs synthesized by Co/Ni catalyst precursors with metallic K. Morphological observations of MWCNTs synthesized by Co/Ni catalyst precursors were shown in Figure 1. Figure 1(a) showed that the MWCNTs have a bamboo-like structure with an average length of 1500 nm. Additionally the inner and outer average diameters of MWCNTs are around 20 and 45 nm, respectively. The inner tube is subdivided by single- or multi-graphite layer, which may be formed by the surface diffusion of carbon cluster on the larger Co/Ni catalytic nanoparticles across the wall of carbon nanotubes. The MWCNTs having irregular-shaped were shown in Figure 1(b). The MWCNTs without amorphous carbon coating typically have open ends when pretreatment processes are carried out with acid- or ultrasonic-purification. As shown in Figures 1(c), the $NaAlH_4$/metal hydrides were well milled and mixed with MWCNTs to form the $NaAlH_4$/MWCNTs nanocomposites. The well-dispersed Pd nanoparticles were also found by impregnation and hydrogen reduction methods shown in Figure 1(d).

Figure 2 represented the metallic K was found in MWCNTs synthesized by Co/Ni catalyst precursors at T = 503-623 K for 12 h and identified with energy dispersive spectrometer (EDS). The postulated equation and reaction mechanism of MWCNTs synthesis may be described as following:
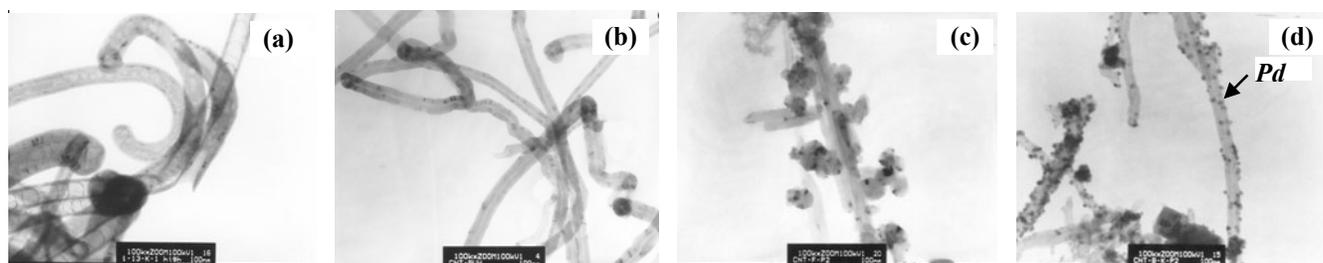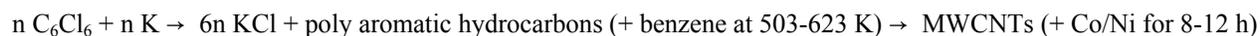
$$n\ C_6Cl_6 + n\ K \rightarrow 6n\ KCl + \text{poly aromatic hydrocarbons (+ benzene at 503-623 K)} \rightarrow \text{MWCNTs (+ Co/Ni for 8-12 h)}$$

Figure 1. TEM images of (a) bamboo-like, (b) irregular- shaped of MWCNTs synthesized by Co/Ni catalyst precursors with metallic K at T = 503-623 K for 12 h, (c) NaAlH$_4$/MWCNTs nanocomposites, and (d) well-dispersed Pd nanoparticles on the surface of MWCNTs

The XRPD pattern shown in Figure 3 indicated that the abstraction of Cl from hexachlorobenzene and formation of the KCl precipitates may be involved in the early stage of the synthesis process of MWCNTs. Since KCl powders can be easily dissolved in water, the high removal efficiency of KCl from MWCNTs samples by washing with water was found (shown in Figures 3 (b) and (c)). KCl was the main species and over 95% of K$^+$ cations was formed as KCl in the synthesis process of MWCNTs by using Co/Ni catalyst precursors at at T = 503-623 K for 8-12 h.
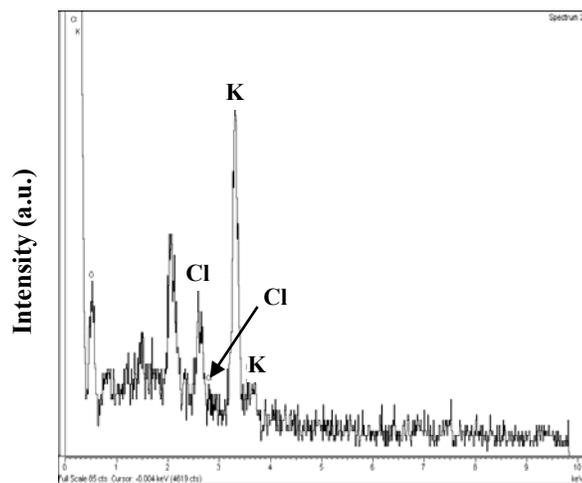

Figure 2. FE-SEM/EDS Measurement of MWCNTs Synthesized by Using Co/Ni Catalyst Precursors with Metallic K at T = 503-623 K for 12 h.
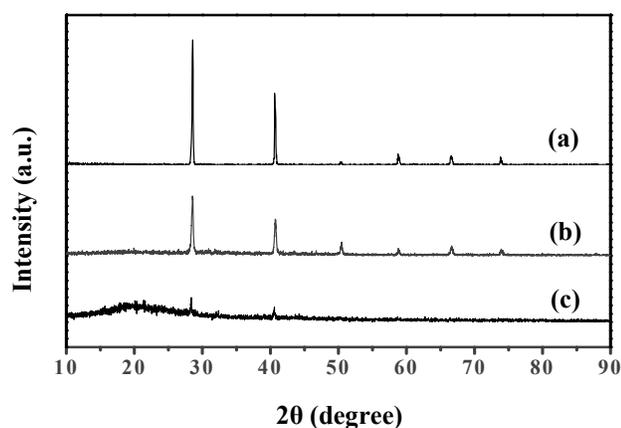
Figure 3. XRPD Patterns of (a) KCl Standard, (b) Unwashed MWCNTs with KCl Crystals, and (c) Washed MWCNTs with KCl Contaminants Synthesized by Co/Ni Catalyst Precursors at T = 503-623 K for 12 h.

Since the valency and fine structure of Co and Ni atom used as the catalyzer precursor of MWCNTs formation had not been well studied, therefore the catalytic redox mechanisms affected by the Co/Ni catalyst precursor in the growth of MWCNTs may be determined by using XANES and EXAFS spectra. Figure 4 showed that the XANES or EXAFS data may indicate the chlorides of Co and Ni were reduced to Co/Ni catalyst particles by metallic potassium, simultaneously hexachlorobenzene was also reduced by potassium through deleting chlorides to form carbon clusters and KCl. By using XANES spectra of Co/Ni precursor residues from the MWCNTs syntheses, all metallic Co or Ni species of the residues are found in Figure 4(a). In addition, all the adsorption curves of Co/Ni precursor residues were compared and confirmed with the ones of metallic Co or Ni powder standards.

The EXAFS data of Co/Ni precursor residues revealed that the nanophase metallic Co or Ni particles had a central Co (or Ni) atom of a coordination number of 2.92 ± 0.05 (or 5.96 ± 0.05) primarily Co-Co with a bond distance of 2.49 ± 0.05 Å

(or 2.48 ± 0.05 Å). These results may offer a further explanation of how the yield and structure of MWCNTs formed by catalytic-assembly benzene-solvothermal route depend on the species of the Co/Ni metal catalysts. However, this result combining with TEM images (Figures 1(a) and 1(b)) might indicate that some MWCNTs having bending structure, and at the close end of the tubes, the catalytic Co/Ni metal particles exist clearly, which may suggest that the Co/Ni metal particles are responsible for the nucleation of the MWCNTs. The concurrence of nucleation of the Co/Ni metal nanoparticles and MWCNTs growth within a reactive hydrocarbon atmosphere (e.g. benzene) creates a complex transient chemical environment, making it difficult to study the inception and growth processes in MWCNTs synthesis.
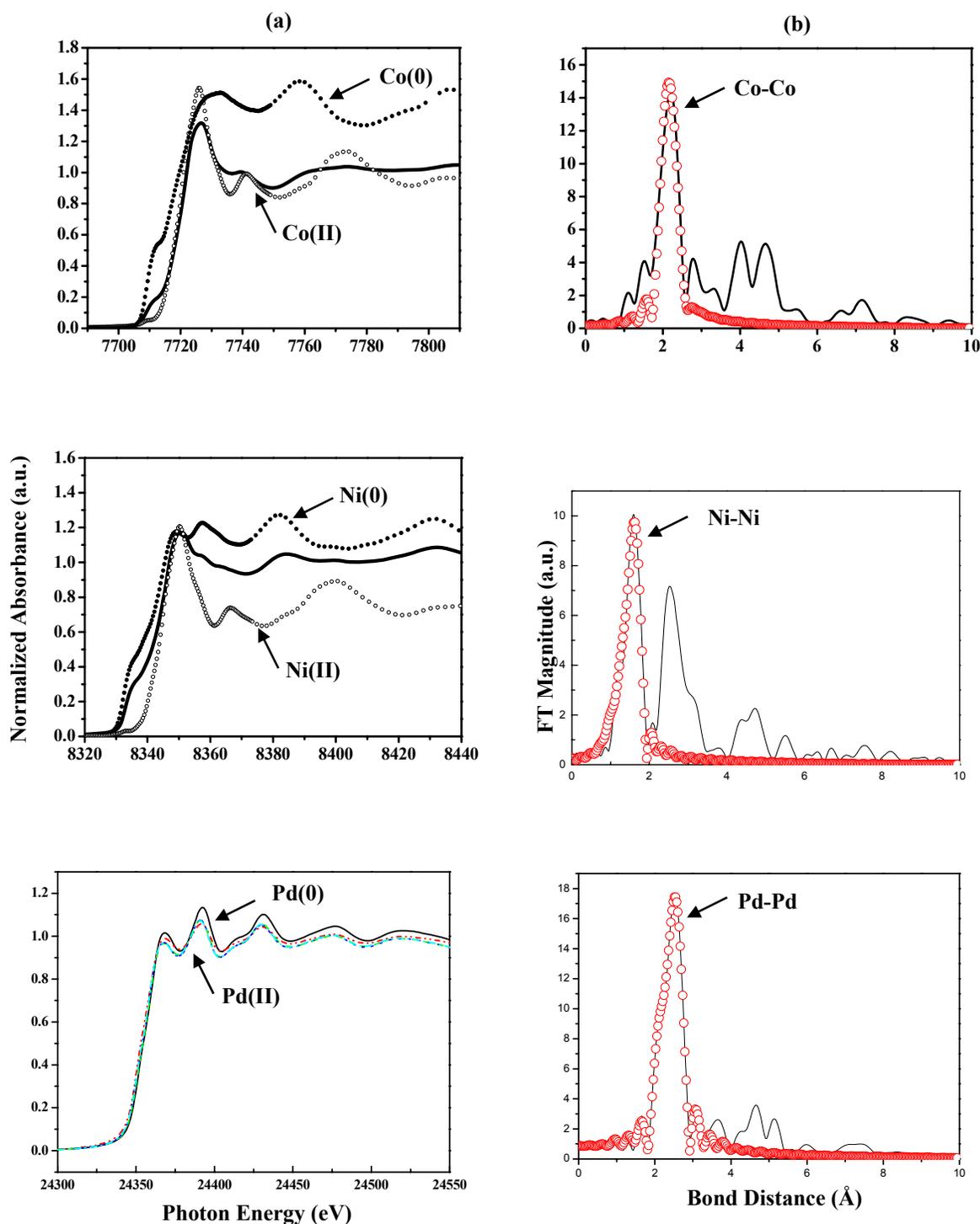

Figure 4. (a) XANES of Co/Ni Precursor Residue Samples (Solid Lines) Compared with Co(0,II), Ni(0,II) or Pd(0,II) Standards and (b) Fourier Transform (FT) of the Metallic Co, Ni or Pd K-Edge EXAFS of the Carbon Nanotubes Synthesized

by Using Co/Ni Catalyst Precursors at T = 603 K for 8-12 h. The Best Fitting of EXAFS Spectra are Expressed by the Dotted Lines.

Since the unique adsorptive properties of carbon nanotubes, it suggests enormous potential applications for MWCNTs on high hydrogen storage efficiency of fuel cell power generation systems. Laboratory-scale experiments were carried out to provide information concerning the feasibility for H_2 storage abilities of MWCNTs, and determined if further developments would be warranted. The chemical modifications of MWCNTs surfaces for adsorption enhancement included HNO_3, $KMnO_4$ and H_2O_2 processes. Moreover, the addition of Pd or $NaAlH_4$ nanoparticles increased the amount of hydrogen adsorbed on MWCNTs. The H_2 storage capacity of MWCNTs improved by Pd or $NaAlH_4$ ranged from 2.5-3.5 wt% shown in Table 1. The Pd/$NaAlH_4$ particles well dispersed on MWCNTs were observed by TEM shown in Figure 1(d). By using EXAFS spectra shown in Figure 4, the Pd clusters possess a Pd-Pd bond distance of 2.76±0.02 Å with a coordination number of 6 and $PdCl_2$ species have a Pd-Cl bond distance of 2.25±0.02 Å with a coordination number of 2. This result revealed that Pd nanoparticles well dispersed on MWCNTs, which may improve the amount of hydrogen storage efficiency significantly.

Table 1. Hydrogen Storage Capacity of MWCNTs, $NaAlH_4$/MWCNTs, and Pd/MWCNTs Nanocomposites.

Adsorbent	Hydrogen Storage Capacity (wt.%)
MWCNTs	0.3-1.0
$NaAlH_4$/MWCNTs Nanocomposite	1.2-2.5
Pd/MWCNTs Nanocomposite	1.8-3.5

Conclusions

The potential synthesis route of MWCNTs with reductive metallic K of catalytic hexachlorobenzene-thermal routes in the presence of Co/Ni catalyst precursors at 503-623 K for 12 h was investigated. The characteristics identification of as-synthesized MWCNTs and H_2 storage capacities of MWCNTs for fuel cell power generation system were also studied. Experimentally, TEM microphotos showed that the MWCNTs have a bamboo-like structure with an average length of 1500 nm. The inner diameter of CNTs is 20 nm and outer diameter 45 nm in average. The XRPD patterns indicated that the abstraction of Cl from hexachlorobenzene and formation of the KCl precipitates may be involved in the early stage of the synthesis process of MWCNTs. From the XANES spectra, the Co/Ni catalyst precursors of the MWCNTs syntheses were all metallic Co or Ni species. Furthermore, the EXAFS spectra of Co/Ni precursor residues revealed that the metallic Co or Ni nanoparticles have a central Co (or Ni) atom of a coordination number of 2.92 ± 0.05 (or 5.96 ± 0.05) primarily Co-Co with a bond distance of 2.49 ± 0.05 Å (or 2.48 ± 0.05 Å). In addition, Pd or $PdCl_2$ possess a Pd-Pd or Pd-Cl bond distance of 2.76 or 2.25 Å with a coordination number of 6 or 2, respectively. The capacity of H_2 storage of MWCNTs improved by Pd or $NaAlH_4$ was ranged of 2.5-3.5 wt%. This result revealed that Pd nanoparticles well dispersed on MWCNTs that may improve the H_2 storage capacity significantly.

Acknowledgement

References

Bahr, J. L., Yang, J., Kosynkin, D. V., Bronikowski, M. J., Smalley, R. E., and Tour, J. M. 2001. Functionalization of carbon nanotubes by electrochemical reduction of aryl diazonium salts: a bucky paper electrode. *J. Am. Chem. Soc.* 123(27):6536-6542.

Branca, C., Frusteri, F., Magazu, V., and Mangione, A. 2004. Characterization of carbon nanotubes by TEM and infrared spectroscopy. *J. Phys. Chem. B* 108(11):3469-3473.

Chaudhuri, S. and Muckerman, J. T. 2005. First-principles study of Ti-catalyzed hydrogen chemisorption on an Al surfaces: a critical first step for reversible hydrogen storage in $NaAlH_4$. *J. Phys. Chem. B* 109(15):6952-6957.

Chen, J., Hamon, M. A., Hu, H., Chen, Y., Rao, A. M., Eklund, P. C., and Haddon, R. C. 1998. Solution properties of single-walled carbon nanotubes. *Science*. 282(5386):95-98.

Conradson, S. D. 1998. Application of X-ray absorption fine structure spectroscopy to materials and environmental science. *Appl. Spectroscopy*. 52(7):252A-279A.

Dillon, A. C., Jones, K. M., Bekkedahl, T. A., Kiang, C. H., Bethune, D. S., and Heben, M. J. 1997. Storage of hydrogen in single-walled carbon nanotubes. *Nature*. 386(6623):377-379.

Dresselhaus, M. S., Dresselhaus, G., and Saito, R. 1995. "Physics of carbon nanotubes. *Carbon*. 33(7):883-891.

Guo, T., Nikolaev, P., Thess, A., Colbert, D. T., and Smalley, R. E. 1995. Catalytic growth of single-walled nanotubes by laser vaporization. *Chem. Phys. Lett.* 243(1-2):49-54.

Hamon, M. A., Hu, H., Bhowmik, P., Niyogi, S., Zhao, B., Itkis, M. E., and Haddon, R. C. 2001. End-group and defect analysis of soluble single-walled carbon nanotubes. *Chem. Phys. Lett*. 347(1-3):8-12.

Hone, J., Zettl, A., and Whitney, M. 1999. Thermal conductivity of single-walled carbon nanotubes. *Synthetic Metals*. 103(1-3):2498-2499.

Iijima, S. 1991. Helical microtubules of graphitic carbon. *Nature*. 354(6348):56-58.

Jiang, Y., Wu, Y., Zhang, S., Xu, C., Yu, W., Xie, Y., and Qian, Y. 2000. A catalytic-assembly solvothermal route to multiwall carbon nanotubes at a moderate temperature. *J. Am. Chem. Soc*. 122(49):12383-12384.

Koningsberger, D., Mojet, B., Miller, J., and Ramaker, D. 1999. XAFS spectroscopy in catalysis research: AXAFS and shape resonances. *J. Synchrotron Rad*. 6(2):135-141.

Liu, J., Shao, M., Chen, X., Yu, W., Liu, X., and Qian, Y. 2003. Large-scale synthesis of carbon nanotubes by an ethanol thermal reduction process. *J. Am. Chem. Soc*. 125(27):8088-8089.

Liu, J., Shao, M., Xie, Q., Kong, L., Yu, W., and Qian, Y. 2003. Single-source precursor route to carbon nanotubes at mild temperature. *Carbon*. 41(11):2101-2104.

Lytle, F. W. 1999. The EXAFS family tree: a personal history of the development of extended X-ray absorption fine structure. *J. Synchrotron Rad*. 6(2):123-134.

Majzoub, E. H., Herberg, J. L., Stumpf, R., Spangler, S., and Maxwell, R. S. 2005. XRD and NMR investigation of Ti-compound formation in solution-doping of sodium aluminum hydrides: solubility of Ti in $NaAlH_4$ crystals grown in HF. *J. Alloy Compd*. 394:265-270.

Mickelson, E. T., Huffman, C. B., Rinzler, A. G., Smalley, R., Hauge, R. H., and Margrave, J. L. 1998. Fluorination of single-wall carbon nanotubes. *Chem. Phys. Lett*. 296(1-2):188-194.

Moc, J., Musaev, D. G., and Morokuma, K. 2003. Activation and adsorption of multiple H_2 molecules on a Pd_5 clusters: a density functional study. *J. Phys. Chem. A*. 107:4929-4939.

Pukazhselvan, D., Gupta, B. K., Srivastava, A., and Srivastava, O. N. 2005. Investigations on hydrogen storage behavior of CNT doped $NaAlH_4$ *J. Alloy Compd*. 403:312-317.

Ross, D. J., Halls, M. D., Nazri, A. G., and Aroca, R. F. 2004. Raman scattering of complex sodium aluminum hydride for hydrogen storage. *Chem. Phys. Lett*. 388:430-435.

Sun, Y. P., Fu, K., Lin, Y., and Huang, W. 2002. Functionalized carbon nanotubes: properties and applications. *Acc. Chem. Res*. 35(12):1096-1104.

Tong, Y., Liu, C., Hou, P. X., Cheng, H. M., Xu, N. S., and Chen, J. 2002. Field emission from aligned multi-walled carbon nanotubes. *Physica B*. 323(1-4):156-157.

Vlaic, G., Andreatta, D., and Colavita, P. E. 1998. Characterisation of heterogeneous catalysts by EXAFS. *Catal. Today*. 14:261-275.

Wang, J., Ebner, A. D., Prozorov, T., Zidan, R., and Ritter, J. A. 2005a. Effect of graphite As a co-dopant on the dehydrogenation and hydrogenation kinetics of Ti-doped sodium aluminum hydride. *J. Alloy Compd*. 395:252-262.

Wang, J., Ebner, A. D., Zidan, R., and Ritter, J. A. 2005b. Synergistic effects of co-dopants on the dehydrogenation kinetics of sodium aluminium hydride. *J. Alloy Compd*. 391: 245-255.

Wang, P. and Jensen, C. M. 2004. Preparation of Ti-doped sodium aluminum hydride from mechanical milling of NaH/Al with off-the-shelf Ti powder. *J. Phys. Chem*. *B*. 108:15827-15829.

Wang, X., Lu, J., Xie, Y., Du, G., Guo, Q., and Zhang, S. 2002. A novel route to multiwalled carbon nanotubes and carbon nanorods atlLow temperature. *J. Phys. Chem. B*. 106(5):933-937.

Wong, S. S., Woolley, A. T., Joselevich, E., Cheung, C. L., and Lieber, C. M. 1998. Covalently-functionalized single-walled carbonn nanotube probe tips for chemical force microscopy. *J. Am. Chem. Soc*. 120(33):8557-8558.

Xing, Y., Li, L., Chusuei, C. C., and Hull, R. V. 2005. Sonochemical oxidation of multiwalled carbon nanotubes. *Langmuir*. 21(9):4185-4190.

Zhang, J., Zou, H., Qing, Q., Yang, Y., Li, Q., Liu, Z., Guo, X., and Du, Z. 2003. Effect of chemical oxidation on the structure of single-walled carbon nanotubes. *J. Phys. Chem B*. 107(16):3712-3718.